Bio-inspired design of flapping-wing micro air vehicles

K. D. Jones
C. J. Bradshaw
J. Papadopoulos
M. F. Platzer
Department of Mechanical and Astronautical Engineering
Naval Postgraduate School
Monterey, CA
USA

ABSTRACT

In this paper the development and flight testing of flapping-wing propelled, radio-controlled micro air vehicles are described. The unconventional vehicles consist of a low aspect ratio fixed-wing with a trailing pair of higher aspect ratio flapping wings which flap in counterphase. The symmetric flapping-wing pair provides a mechanically and aerodynamically balanced platform, increases efficiency by emulating flight in ground effect, and suppresses stall over the main wing by entraining flow. The models weigh as little as 11g, with a 23cm span and 18cm length and will fly for about 20 minutes on a rechargeable battery. Stable flight at speeds between 2 and 5ms^{-1} has been demonstrated, and the models are essentially stall-proof while under power. The static-thrust figure of merit for the device is 60% higher than propellers with a similar scale and disk loading.

NOMENCLATURE

c	aerofoil chord length
C_p	coefficient of power
C_t	coefficient of thrust
f	frequency in Hz
k	reduced frequency, $2\pi fc/U_\infty$
L/D	lift over drag ratio
U_∞	freestream velocity
x	streamwise coordinate
z	cross-stream coordinate
α	angle-of-attack in degrees
η	Propulsive efficiency, C_t/C_p
ϕ	Phase angle in degrees

1.0 INTRODUCTION

The brilliant success of organisms which achieve flight using flapping-wing propulsion has been an inspiration to humankind for hundreds if not thousands of years. This has led to the, perhaps erroneous, belief that flapping-wings are superior to other forms of propulsion. The justification for this belief is that nature has chosen flapping-wings through natural selection. Of course this argument is rather naive, as it ignores the initial conditions and constraints of the evolutionary process. In truth, one does not find many rotating parts in nature, and therefore a reasonable argument is that nature did not select flapping wings over propellers, but rather propellers were excluded from the process entirely.

However, there are several arguments supporting flapping-wing propulsion which do hold merit. For example, rotary propellers generate torque and create helical slipstreams, both of which degrade vehicle performance and handling, particularly at low speeds. Additionally, flapping-wings may easily have a larger actuator area,

Paper No. 2950. Manuscript received 11 January 2005, accepted 18 July 2005.

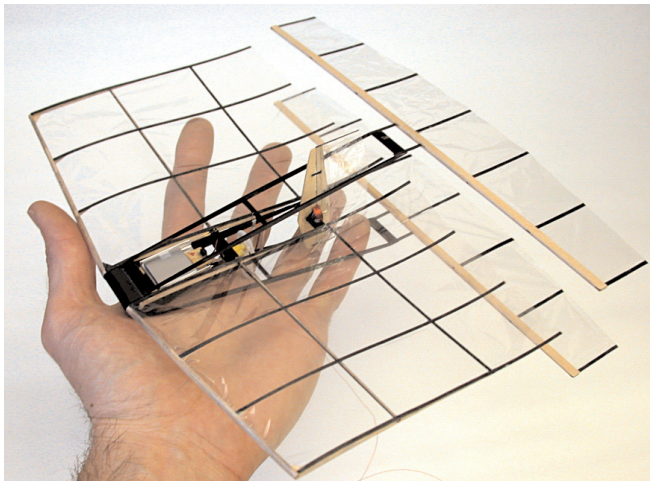

Figure 1. NPS flapping-wing MAV.

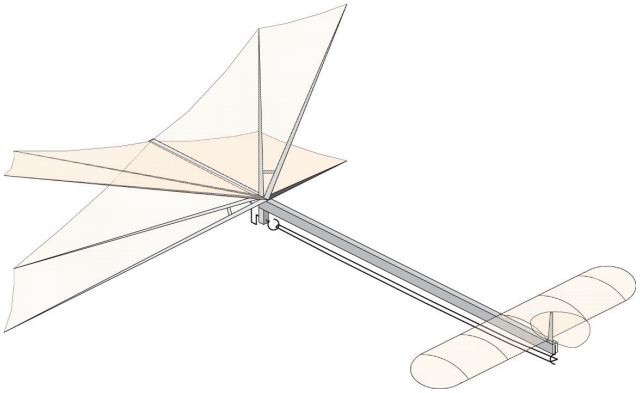

Figure 2. Frank Kieser's winning X-wing flapper.

and therefore a lower actuator loading, which may lead to increased efficiencies. On the other hand, flapping-wings have inherent mechanical losses and increased structural loads. The structural and inertial requirements likely limit flapping-wing propulsion to smaller scales, however, at these smaller scales low Reynolds number effects further complicate the problem, for both conventional and flapping-wing propellers.

Many have argued about the relative merits of fixed, flapping or rotary-wing design, see for example Woods *et al*[1]. While most in the micro air vehicle (MAV) community have concentrated on fixed-wing aircraft, the capabilities of flapping-wing designs in nature, which can hover, maneuver in tight spaces, and even land on a ceiling, greatly exceed anything humankind has been able to produce, and this alone is motivation enough to pursue flapping-wing flight.

The creativity, ambition and persistence of countless enthusiasts have led to a variety of successful flapping-wing flyers over at least the past 130 years. These designs are often classified as either biomimetic (a design which mimics nature) or biomorphic or bio-inspired (a design which is inspired by nature, but is not a copy of nature). The configuration developed in this investigation, shown in Fig. 1, clearly falls into the second category.

1.1 Biomimetic designs

Flapping-wing model aircraft date back at least to 1874, when Alphonse Penaud built a rubber-band powered ornithopter. Since then, with just a few exceptions, almost all successful flapping-wing aircraft have been biomimetic, at least for the flapping-wings. Probably the most well known biomimetic flapper in the aerospace community is AeroVironment's Microbat. Their philosophy was to take a functional rubberband powered design and substitute an electrical motor drive-train for the rubberband and add a radio for control[2]. They make an interesting note, stating that the specific energy of the rubberband is comparable to that of the motor/gearbox/battery/DC-DC-converter assembly. In 2003, a version of the Microbat using a two-cell Lithium-polymer (Li-poly) battery, three channel radio, and with a 23cm span and 14g total weight, reportedly made a flight of about 25 minutes.

1.2 Biomorphic designs

Projects like the Microbat clearly demonstrate that biomimicry can lead to success, but one is left to ponder whether or not there is a better way. For example, model airplane enthusiasts have been building rubberband powered ornithopters for more than a century, and to date, the greatest endurance has been achieved by something that did not look at all like a bird, using instead a biplane flapping mechanism, as shown in Fig. 2. The biplane or X-wing canard flapper, built in 1985 by Frank Kieser, set a new record for indoor free flight endurance[3]. Variations of this design still hold the record. While the model does not appear to look like anything in nature, in fact, the flapping of its wing-pairs is much like a bird flying in ground effect.

Following a similar path, a collaboration between SRI and the University of Toronto produced the Mentor, reportedly the first flapping-wing aircraft to hover under its own power[4]. Like Frank Kieser's design, the Mentor is designed to capitalise on the Weis-Fogh or clap-and-fling effect, and seems to be designed primarily for hovering flight – a flapping-wing helicopter of sorts, although forward flight has also been demonstrated. Neither design looks anything like a bird or insect, but many birds and insects make use of the Weis-Fogh effect and were an inspiration for these designs.

We have found it instructive to try to discern which aspects of animal morphology evolved as a result of organic and/or environmental limitations, and which aspects are performance enhancing. While this is not always simple, one approach we have found useful is to look at how animal behavior is used to compensate for design limitations. For example, birds have evolved with a single pair of wings, so configurations such as the model shown in Fig. 2 are not possible. However, the fact that birds fly low over the ocean indicates that birds have indeed discovered the benefits of flapping in ground effect, a behaviour that makes them aerodynamically similar to the X-wing configuration. The exploitation of ground effect is one of the behavioral adaptations which are utilised in this investigation.

For the present design, much of the development process has been documented over the years in AIAA papers and other publications. A fairly detailed summary of our past work can be found in Jones *et al*[5] and Jones and Platzer[6], with references to most of our other publications. In this paper the history is briefly summarised, with more details provided on progress made since the earlier publications, and some summarising remarks on what the future might bring.

2.0 DESIGN PHILOSOPHY

As previously mentioned, much can be learned from observations of animal flight, but care must be taken to determine which features have evolved to enhance performance, and which were forced due to organic or environmental constraints. For example, a bird flaps its

https://doi.org/10.1017/S0001924000000804 Published online by Cambridge University Press

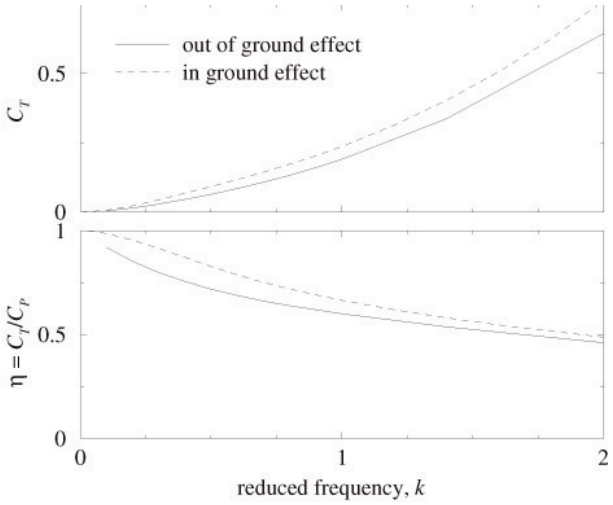

Figure 3. Predicted benefits of ground effect.

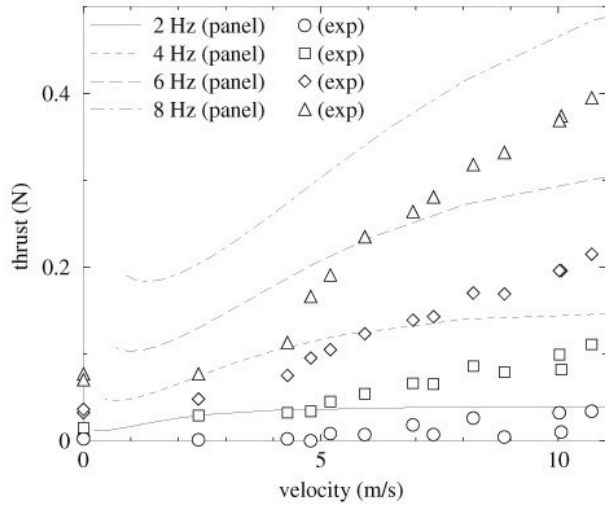

Figure 4. Thrust measurements in ground effect.

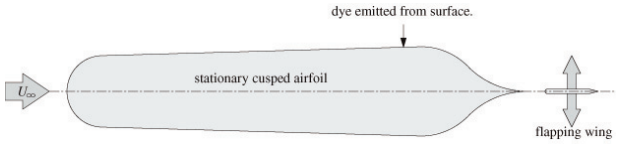

Experimental schematic.

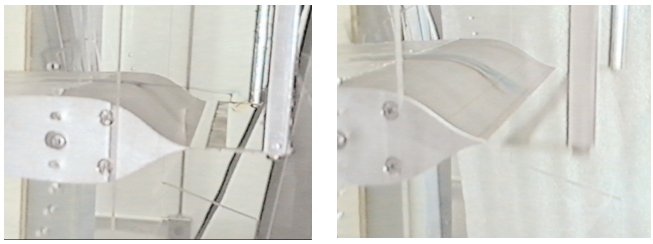

Static – dye indicates separation Flapping – dye indicates eattachment

Figure 5. Flow reattachment due to flow entrainment.

wings such that the flap-amplitude varies along the span. This does not appear to be an optimal arrangement, but the bird does not have an alternative. We would prefer to flap the wing with constant amplitude to produce thrust from the root section of the wing, and to provide for a more efficient span loading.

In the early years of our research, significant effort was directed toward simulations of fairly basic flapping-wing mechanics in an effort to better understand the complicated unsteady flow phenomena, and with the hope of developing numerical tools to aid in a design optimisation methodology. Unsteady panel methods were developed in conjunction with flow visualisation and laser Doppler velocimetry (LDV) measurements in wind and water tunnels[7-10], and several significant conclusions were made.

First, the benefit of flapping in ground effect was quantified, both numerically and experimentally, as shown in Figs 3 and 4. For these simulations, an airfoil was plunged sinusoidally at zero angle of attack, with the specified frequency, and with plunge amplitude $0.4c$. The ground-effect simulations were modeled using an image airfoil below ground, with a mean separation of $1{\cdot}4c$, corresponding to a mean distance from the ground of $0{\cdot}7c$. The experimental measurements were performed on a biplane model, where the two wings flapped in counterphase, essentially duplicating the panel-code model – emulating ground effect through symmetry. A 5 to 10% increase in both the thrust coefficient and propulsive efficiency were predicted. Additionally, the agreement between experiment and the panel code were quite good, particularly for the low experimental Reynolds numbers (less than 5×10^4).

A secondary benefit of the biplane arrangement was that the model, as a whole, was dynamically balanced, minimising vibrations of the apparatus. While dynamic balancing was convenient for testing in a wind-tunnel, it appeared to be even more advantageous for a flying model. Flapping a single wing in flight would result in oscillations of the fuselage – work done with no gain in performance. However, by flapping two wings in counterphase, the fuselage would remain steady, and all the work would be used to move components which directly produce thrust.

It is likely that birds have evolved to compensate for this imbalance. Their neck is highly articulated, such that their head is inertially stable for improved vision, and their body and tail most likely create additional thrust as they oscillate in opposition to the wing motion. However, it is doubtful that any man-made ornithopters benefit from fuselage oscillations, as this requires a level of sophistication beyond our current capabilities.

Another aerodynamic phenomenon we wished to exploit was the ability to suppress flow separation using the flapping wings. Dynamic stall delay due to oscillatory pitching is a fairly well known phenomenon, of particular interest to rotary-wing engineers[11,12]. However, a lesser known application is the use of a flapping wing downstream of a larger airfoil, using the favorable pressure gradient ahead of the flapping wing to suppress flow separation on the larger wing. Water-tunnel experiments demonstrated this phenomenon for flow over a backward-facing step[8], and for separation control of flow over several blunt trailing edge airfoils[9,13], as shown in Fig. 5.

In the upper image the general experimental setup is shown, illustrating a large, stationary airfoil with a cylindrical leading edge and a rather abrupt cusped trailing edge. The airfoil thickens slightly along the chord to keep the boundary layer thin. Dye is emitted from a small hole just upstream of the cusped trailing edge region, where the flow is expected to be attached. Following the stationary wing is a small wing which may be flapped. The lower images show experimental snapshots. In the left image the trailing wing is stationary,

https://doi.org/10.1017/S0001924000000804 Published online by Cambridge University Press

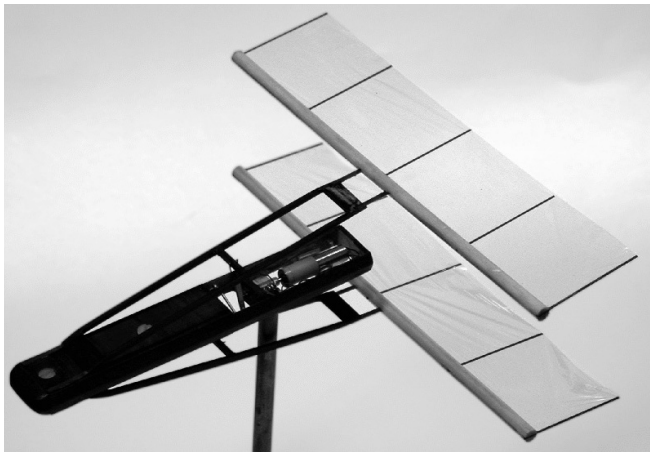

Figure 6. 15cm length/span MAV propulsion model.

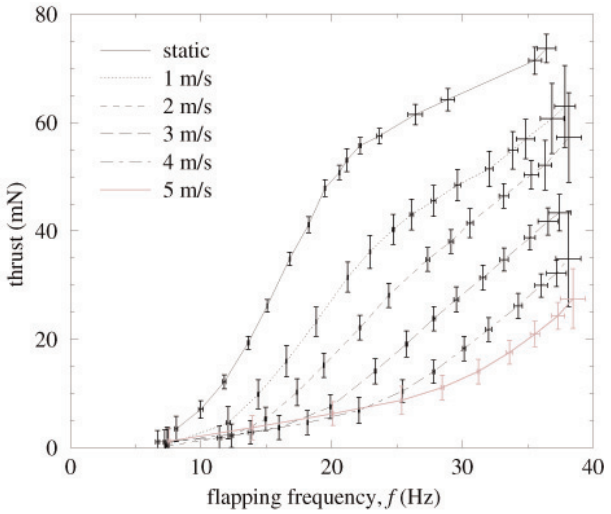

Figure 7. Performance of the propulsion model.

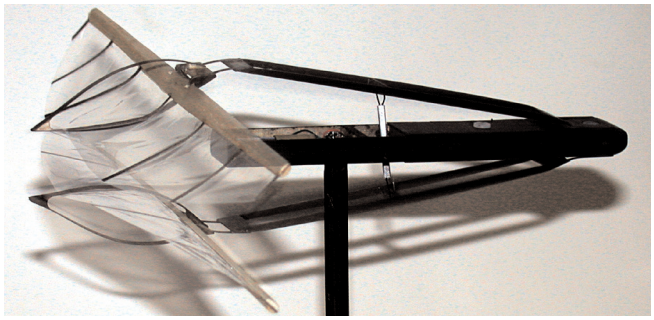

Figure 8. Aeroelastic cambering wings.

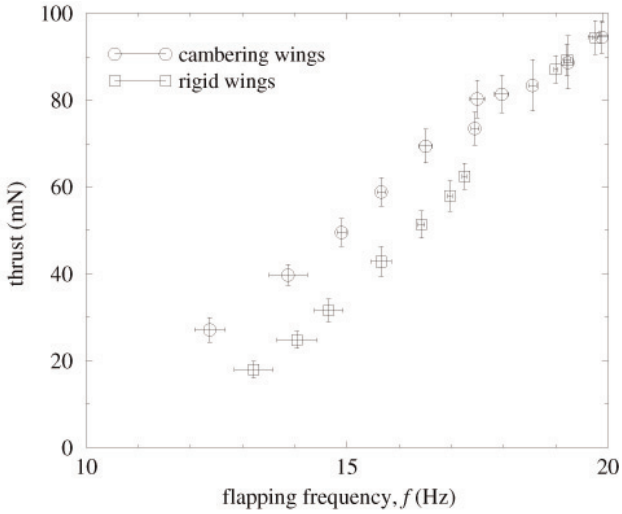

Figure 9. Static performance of cambering wings.

and the flow completely separates at the onset of the recompression. In the right image, with the trailing wing flapping, the dye indicates that the flow has reattached.

It was hoped that a similar success might be realised on a flapping-wing MAV. This facet is of particular interest for low speed MAVs, as the flight Reynolds numbers may be quite low, on the order of 2×10^4, where the flow is laminar, and separation is likely.

These considerations led us to the configuration shown in Fig. 1, with a biplane-pair of trailing wings, flapping in counterphase, coupled with a large fixed wing located just upstream of the flapping wings.

3.0 DESIGN METHODOLOGY

As previously mentioned, the early years of our research were focused on developing simulation software which might be used in an optimisation algorithm to design an efficient flapping-wing MAV. Unfortunately, what our research demonstrated was that the low Reynolds numbers led to flow physics which could not be adequately predicted using inexpensive methods such as our panel code. Simulations with a two-dimensional unsteady Navier-Stokes solver provided much better agreement with experimental measurements[10,14], but were far too costly to be embedded as part of an iterative design process. Therefore, in the end we had to resort to a more hands-on or heuristic approach, using failures and successes to drive the evolutionary design process.

3.1 Mechanics of thrust generation

One of the first lessons to be learned was simplicity in design. On a large model complicated mechanisms could be developed to add several degrees of freedom to a flapping mechanism. However, working on a MAV-scale, size and weight issues dominated, and the flapping mechanism had to be reduced to a single active degree of freedom – plunge. Test models, like the one shown in Fig. 6 were assembled, allowing for the direct measurement of thrust, and it quickly became apparent that a pitch degree of freedom was necessary. To keep things mechanically simple, this was done passively by attaching the flapping wings to the flapping mechanism with a flexible joint so that they were able to pitch aeroelastically. Typical performance from the models is shown in Fig. 7.

Inspired by Cylinder *et al*[15], a second passive degree of freedom was attempted – camber. The model is shown in action in Fig. 8, with the flash-frozen wings shown at mid-stroke as they pulled away from each other. An elastic angle of attack of about 30° is visible, as well as the fully cambered wing. The measured performance of the cambering wings is shown in Fig. 9. While the camber provided excellent and predictable performance for lower frequencies, at higher frequencies the wings did not have enough time to change

https://doi.org/10.1017/S0001924000000804 Published online by Cambridge University Press

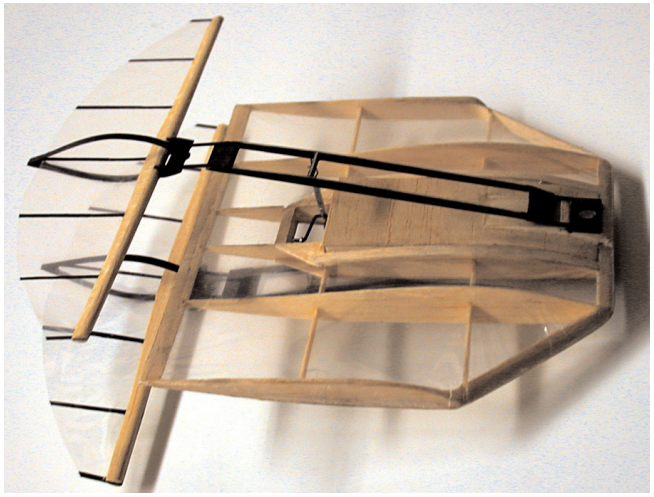

Figure 10. First fixed/flapping-wing configuration.

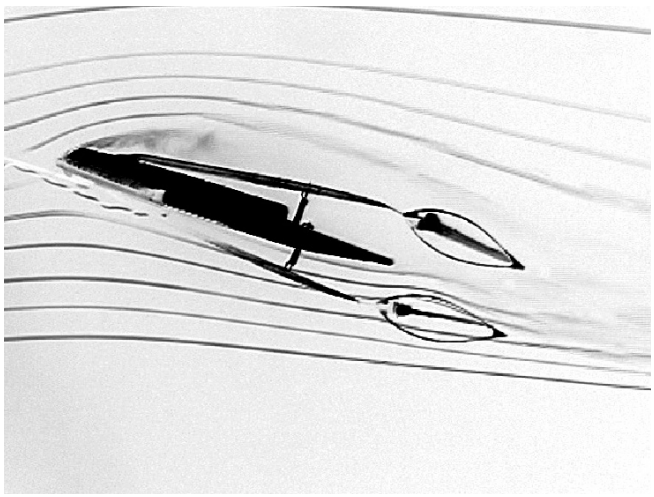

Static

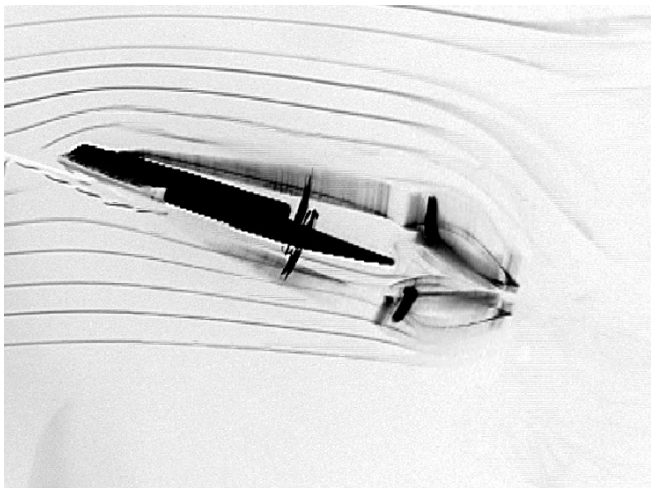

Flapping

Figure 11. Separation control at high AOA.

camber, and the performance degraded to that of the flat-plate wings. With some additional work, perhaps this too could be resolved, but due to the added weight and complexity of the cambering wings, for the time being they were eliminated from the design.

All of these early test models used tiny, geared stepping motors, which required large external power supplies and controllers. While these drive systems were desirable for wind-tunnel models, they were not suitable for flying models, and they were replaced by brushed DC motors with custom gearboxes for the following models.

3.2 Lift generation

The next step was the integration of the flapping-wing pair with a fixed leading wing. The first test model, shown in Fig. 10, still conformed with DARPA's 15cm square size criteria. This model was tested in the wind-tunnel, and using flow visualisation with a smoke wire, provided the first evidence of separation control using the flapping wings. This is illustrated in Fig. 11, where the wings are not flapping on the upper image, with the flow separating at the leading edge, and on the lower image, with the wings flapping, the flow appears to have reattached.

Tethered flight on a radial-arm test stand indicated that speeds on the order of 2 to 3ms^{-1} were possible while generating enough lift to support the 7g weight. At that time commercial-off-the-shelf (COTS) batteries and radio gear added up to a minimum of about 20g, so untethered flight was not feasible.

3.3 Energy storage

We are fortunate that some of the critical components we use are also critical to the cell-phone industry, and hence performance improvements have been tremendous; specifically, batteries, motors (the motors that vibrate pagers and cell-phones), and DC-DC converters to step-up a low voltage.

Battery technology has been driven by the cell-phone industry at an extreme pace. Five years ago, about the best solution was a 50mAh nickel cadmium cell, providing 0·06Wh in a 3·5g cell – an energy density of about 17Wh/kg. The rechargeable Li-poly cells we use now have a capacity of 135mAh and can provide 0·5Wh. Weighing a mere 3g, they have an energy density of about 170Wh/kg, or ten times what the NiCd cell provided.

3.4 Motor/gear assembly

The motors are currently one of the weakest links. While the cell-phone industry has pushed hard to make small, light and cheap motors, they have done little to improve the efficiency. The motors we used (Didel MK06L-10 or MK06-04.5) weighed about 1.3 to 1·5g, and used a two-stage gear system. For the first models we had to fabricate our own gear systems, but now we use gear assemblies built for the indoor model aircraft hobbyist (Didel 6R21). Using a miniature dynamometer we measured the efficiency of the motor/gear assembly, and at flight loads it was below 25%.

On the other hand, the motor/gear assemblies were very light, about 2·2 to 2·5g, and they were able to deliver more than 0.4W of shaft power, a power density of 180W/kg, which is quite good for this scale.

3.5 Power conversion

A variety of motors were available, with nominal voltages between 0·8 and 2·4V. The first flying models built used motors designed for 1·2V with a rated power output of about 0.14W. In order to achieve

https://doi.org/10.1017/S0001924000000804 Published online by Cambridge University Press

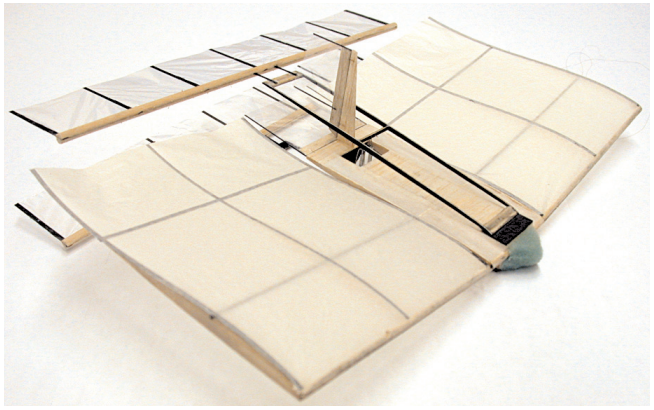

Figure 12. First flying model.

the power required to fly the MAV, we needed to increase the power output considerably, and this was done by running the motor at a much higher voltage. A miniature DC-DC step-up circuit was assembled to bump the 3·0 to 4·2V from the battery up to a regulated 5V. The circuit was based on an IC designed for cell-phone type devices, but was miniaturised as much as possible, with some sacrifice in efficiency. The circuit weighed about 0.35g, and produced a regulated 5V supply up to about 0·5A.

With some of the lower resistance motors now available, the power converter is not required; although the flight performance degrades somewhat as the battery life is exhausted and the voltage drops.

3.6 Avionics

The radio gear is COTS hobbyist equipment, designed for park-flyers and indoor model aircraft. The three channel receiver (Slowfly RFFS-100) weighs about 2g, slightly less if you remove the bulky connector pins it comes with, and it includes an electronic speed control and drivers for two magnetic actuators. The receiver is not narrow band, and is limited to about 100m range.

The magnetic actuators are comprised of small coils and a magnet pair. The coil is glued to the aircraft frame, and the magnets are glued to the control surface, such that they are inside the coil. When the coil is energised, the magnets try to align with the coil field, deflecting the control surface. If the control surface is lightly spring loaded to return to center, then proportional control can be achieved by varying the duty cycle of the coil.

The actuators are the other weakest link. They are not light, typically 0·7 to 1g each, and they are not efficient, drawing as much as 0·5W each, but they are relatively inexpensive, easy to use and quite durable.

3.7 Vehicle sizing

The next step in the design procedure was to size the configuration for the required payload, in this case, just the propulsion and control system. The components we used on our first model were slightly heavier than those listed above, adding up to about 9·25g for a battery, converter, drive system and receiver. From past building experience, we estimated the weight of the structure to be about 5g, yielding a total weight of just over 14g.

While little experimental data was available for low aspect-ratio wings in the 2×10^4 to 5×10^4 Reynolds number range, papers by Laitone[16] and Torres and Mueller[17] suggested that lift coefficients on the order of about 0·6 were possible with an L/D_{max} of around 5 on an aspect-ratio 2 wing. This indicated that a wing area of about 0·06m^2 was needed.

4.0 DESIGN EVOLUTION

The first model, shown in Fig. 12, flew in December of 2002. It had a main wing with a 30cm span and 14·5cm chord, and flapping wings with a 25cm span and 4cm chord. It used a single-channel control, throttle-only, with fixed rudder trim for a shallow turn, and fixed pitch trim to give it a constant nose-up attitude. The flying weight was about 14·4g, and the model made a number of flights, the longest lasting about three minutes before coming to rest high up in a tree.

Flight speed was only about 2ms^{-1}, and the ability of the model to fly at very high angles of attack without stalling suggested that separation control was in effect. With the power off, the model would stall quite easily in response to gusts, but under power, it would merely settle back into level flight without loosing any altitude.

Several months later a second model was built; slightly smaller, with a 27cm span, and including a rudder control. The weight was reduced to 13·4g, and the model could now sustain longer flights, as trees and buildings could be avoided. During an AIAA technical seminar at NASA Ames on 12 February 2003, the model was flown in the test section of the 80 by 120ft NFAC tunnel – one of the smallest aircraft flying the world's largest wind-tunnel.

The second model was still without elevator control, so it was trimmed with a nose-up attitude, and throttle was used to control rate-of-climb. By changing the pitch trim, the flight speed could be adjusted. The model flew well from speeds as low as 2ms^{-1} up to about 5ms^{-1}. Higher speeds would be possible with active pitch control, but were risky with a preset pitch trim, as the model might easily dive into the ground in response to a gust.

A Watt-meter was attached to the model on the bench top, and at full power 1·5W was drawn from the battery while the model produced about 10g of static thrust. Considering only the motor/gear efficiency (ignoring losses through the DC-DC converter, receiver/speed-controller, and crankshaft assembly), this suggests that about 0·375W shaft power was delivered, resulting in a figure of merit (FOM) of about 30g/W at an effective disk-loading of about 6N/m^2. This is about 60% higher than comparable rotary wing vehicles[18].

Table 1
Model details

Model	Span	Length	Avionics weight	Battery weight	Motor/gear weight	Structural weight	Total weight
1	30cm	20cm	2·7g	3·8g	2·7g	5·2g	14·4g
2	27cm	19cm	3·1g	3·2g	2·5g	4·5g	13·4g
3	25cm	18cm	2·7g	3·2g	2·3g	4·2g	12·4g
4	23cm	17cm	2·7g	2·3g	2·3g	3·8g	11·0g

https://doi.org/10.1017/S0001924000000804 Published online by Cambridge University Press

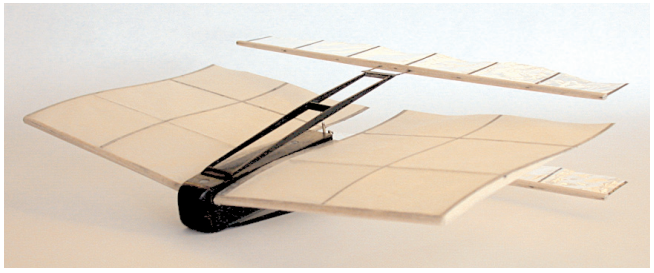

Figure 13. Wind-tunnel variant of the MAV.

A third model, shown previously in Fig. 1, is slightly smaller yet, with a 25cm span and 12·4g flying weight. It uses a lower voltage motor, eliminating the need for the DC-DC converter, and it has interchangeable parts allowing for more systematic optimisation. The main wings on this model incorporate about 5° of leading-edge sweep and a reduced dihedral-angle. The yaw-roll coupling on the third model is higher than the previous models allowing for a very tight turn radius, even without active pitch control.

A fourth model was assembled to compete in the 8th International MAV competition, in April 2004. It had an even smaller span (as well as the longest linear dimension) of 23cm, and weighed just 11g. A summary of model dimensions and weight breakdown is shown in Table 1.

5.0 DESIGN ANALYSIS

With flying models in hand, we now went back to the wind-tunnel in order to gain a better understanding of the flow physics; hopefully allowing us to optimise the design. Since the pager motors used in the flying models had a relatively short lifespan, a model was built with the same fixed and flapping-wing geometry as the second radio controlled model, but with a larger fuselage to house a bigger motor and rotary encoder and with interchangeable parts. The new model, shown in Fig. 13, was attached to a two-component force balance to measure lift and thrust, and flow visualisation and unsteady LDV experiments were run.

5.1 Flow visualisation

Streaklines were generated by a smoke wire which was constructed from 0·25mm diameter NiCr beaded wire, heated by passing a current through it, and using Rosco Fog Juice as the smoke agent. Imagery was recorded using either a digital still camera or a digital video camera with a high shutter speed to freeze the motion of the wings and streaklines. Details of the methods can be found in Jones and Platzer[6] and Papadopoulos[19].

Flow visualisation experiments were performed with the model mounted at a 15° angle of attack, at a flow speed of about 2ms^{-1}, approximating the low-speed flight conditions. Initially the flapping wings were at rest, and they were then quickly accelerated to a flapping frequency of about 30Hz. The results are shown in Fig. 14, viewing the model from the left rear corner forward; an angle which provides a good view of the flow over the upper surface of the left wing. In the upper image, without wing flapping, it is clearly seen that the flow separates at the leading edge, and the wing is fully stalled. In the upper image, after just four flapping strokes, the flow is already reattached. While the boundary layer appears to be very thick and unsteady, the outer flow remains parallel to the upper wing surface and reattaches at the trailing edge. Not only is the flow entrainment sufficient to reattach the flow, but it requires only about a tenth of a second to transition. The Reynolds number is about 2×10^4 for the main wing, and just 5×10^3 for the flapping wings.

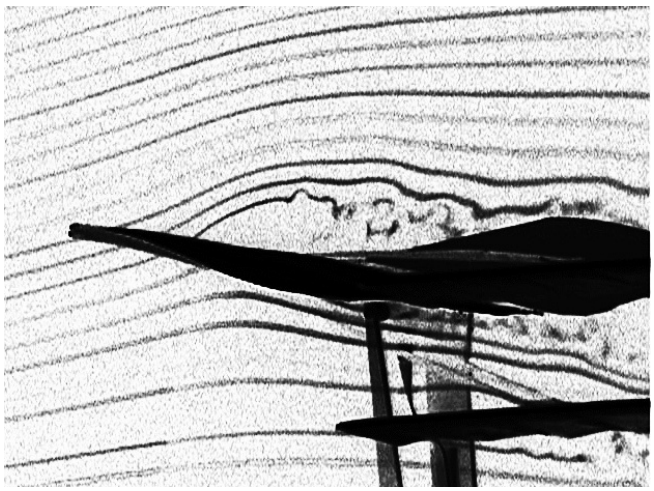

Static

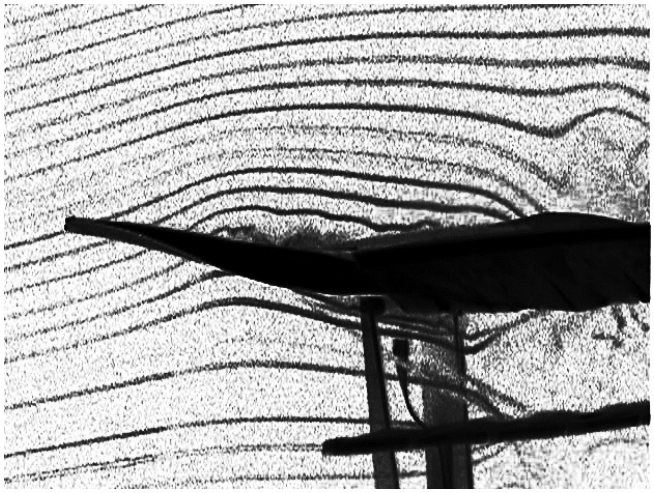

Flapping

Figure 14. Separation control at high AOA.

5.1 Laser-doppler flow measurements

A TSI two-channel LDV system with a single probe was used, with flow seeding provided by a Rosco fog generator. For unsteady measurements, the signal from the rotary encoder was fed into a rotary motion resolver (RMR), which allowed the LDV system to record periodic data, synchronised with the wing flapping. Further details about the setup and measurement procedures can be found in Bradshaw[20].

Use of the RMR provided for higher fidelity velocity measurements, removing the effects of phase-biased flow seeding. Since LDV is a statistical average of a large number of recorded events, in an unsteady, periodic flow, the seeding density may fluctuate periodically, biasing the velocity prediction toward the more heavily seeded parts of the cycle. This biasing was removed using the RMR, resulting in somewhat higher velocity peaks.

The flow-entrainment effect is illustrated in Figs. 15 and 16. In Fig. 15 the time-averaged velocity profile just in front of the flapping wings ($x = 0$) is shown for three cases. In the first case, the main wing is removed, and the wings are flapped at 32Hz. In the second case the

https://doi.org/10.1017/S0001924000000804 Published online by Cambridge University Press

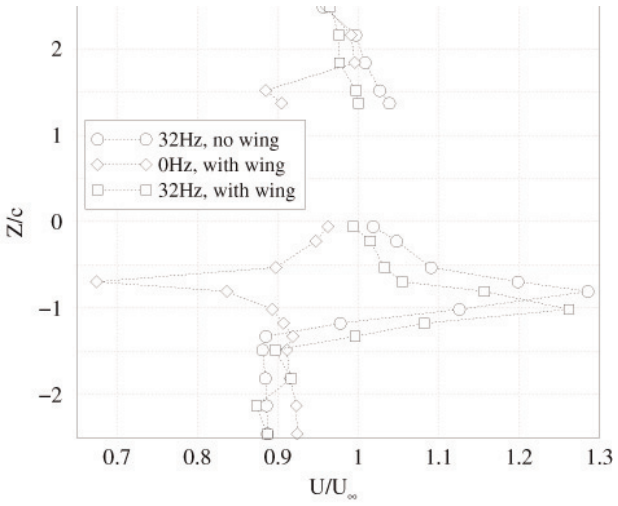

Figure 15. Time-averaged velocity at $x = 0$.

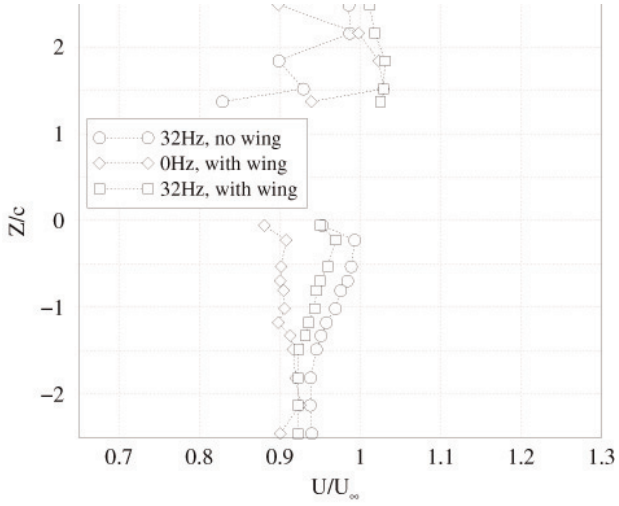

Figure 16. Time-averaged velocity at $x = -c$.

main wing is included, but the wings are not flapped. In the third case, the main wing is included and the wings are flapped at 32Hz. In all three cases the freestream speed is 2·75ms^{-1}, and the model is set at a 15° angle of attack. Unfortunately, the dihedral of the main wing masked a large area above the symmetry plane, roughly where the figure legend is placed, such that the effect of the upper flapping wing is partially obscured.

Comparing the flapping cases with and without the main wing, the entrainment effect is clearly seen with about a 30 percent over-velocity at the centerline of the lower flapping wing. Note that the velocity profile is nearly unaffected by the inclusion of the main wing. Without flapping the wings, a large velocity deficit is seen near the stagnation point on the leading edge of the lower flapping wing. Also note that without flapping the wings, a velocity deficit appears more than a chordlength above the main wing, illustrating the severity of the separated flow.

In Fig. 16, velocity profiles a chordlength upstream of the flapping wings ($x = -c$) are shown for the same three cases, and it can be seen that the entrainment effect has diminished considerably, indicating that the flapping wings must be quite close to the trailing edge of the main wing to capitalise on this phenomenon.

6.0 SUMMARY & PROSPECTIVE

Almost a decade of research in flapping-wing propulsion and low Reynolds number unsteady aerodynamics has culminated in the development of an unusual flapping-wing propelled micro air vehicle. The configuration consists of a biplane pair of flapping wings, which move in counterphase, located just downstream of a fixed wing. The relatively large fixed wing provides most of the lift, while the flapping-wings provide the thrust and suppress flow separation on the main wing due to their flow entrainment. The symmetry of the flapping-wing pair provides mechanical and aerodynamic balancing, and produces thrust more efficiently than conventional flapping-wing systems.

The present model, using commercial off the shelf power and avionics equipment, has a 25cm span, 18cm length and weighs a paltry 12·4g, with two-channel control and enough battery capacity for 15 to 20 minutes of flight. The model does not have active pitch control, but the pitch may be manually trimmed to set the flight speed. Speeds between about 2 and 5ms^{-1} have been achieved, and the model is virtually stall-proof while under power, due to the separation suppression characteristic of the design.

Wind-tunnel measurements of lift and thrust, as well as flow visualisation and unsteady LDV measurements of the surrounding flowfield have verified the flow separation suppression phenomenon, and now provide a means for the systematic analysis of the design, which will eventually allow for design optimisation. While the current design flies extremely well, it is by no means optimised. However, operating with a static figure of merit of almost 30g/W, it exceeds low Reynolds number (5×10^3 to 2×10^4) propeller performance at an equivalent disk loading by at least 60 percent. Furthermore, the design should scale down well, allowing for much smaller vehicles as power and avionics technology improves.

While there are several natural directions for the project to evolve, its low speed performance makes it highly suitable for missions where flight in confined areas is required. It is likely that the flight speed can be reduced much further, perhaps eventually achieving hovering flight. Along with the low flight speed comes the ability to park the vehicle in strategic places, allowing it to gather and transmit data long past its useful flight lifetime. There are certainly many other possibilities, limited only be our creativity and perseverance.

Research is currently underway to investigate the complicated interaction between the three wings. Low Reynolds number Navier-Stokes analysis of the aeroelastic pitching mechanism is in progress, as well as simulations of the bi-plane interaction of the flapping wings. Future work will include all three wing sections in order to simulate the flow-entrainment and reattachment phenomenon.

ACKNOWLEDGMENTS

We are grateful for the support received from Richard Foch, head of the Vehicle Research Section of the Naval Research Laboratory, and project monitors Kevin Ailinger, Jill Dahlburg and James Kellogg.

REFERENCES

1. WOODS, M.I., HENDERSON, J.F. and LOCK, G.D. Energy requirements for the flight of micro air vehicles, 2001, *Aero J*, **105**, (1045), pp 135-149.
2. KEENNON, M.T. and GRASMEYER, J.M. Development of the Black Widow and Microbat MAVs and a vision of the future of MAV design, 2003, AIAA Paper No 2003-3327.

https://doi.org/10.1017/S0001924000000804 Published online by Cambridge University Press

3. CHRONISTER, N. Ornithopter media collection, 2001, http://www.ornothopter.org/rubber.html.
4. BRIDGES, A. Flying robots create a buzz, *Monterey County Herald*, 28 July, 2002.
5. JONES, K.D., LUND, T.C. and PLATZER, M.F. Experimental and Computational Investigation of Flapping-Wing Propulsion for Micro Air Vehicles, 2001, Chapter 16, *Fixed and Flapping Wing Aerodynamics for Micro Air Vehicle Applications*, AIAA Progress in Aerospace Sciences Series, MUELLER, T. (Ed), **195**.
6. JONES, K.D. and PLATZER, M.F. Experimental investigation of the aerodynamic characteristics of flapping-wing micro air vehicles, AIAA Paper No 2003-0418, 2003.
7. JONES, K.D., DOHRING, C.M. and PLATZER, M.F. An experimental and computational investigation of the Knoller-Betz effect, *AIAA J*, 1998, **36**, (7), pp 1240-1246.
8. LAI, J.C.S., YUE, J. and PLATZER, M.F. Control of backward facing step flow using a flapping airfoil, *Experiments in Fluids*, 2002, **32**, pp 44-54.
9. DOHRING, C.M., FOTTNER, L. and PLATZER, M.F. Experimental and numerical investigation of flapping wing propulsion and its application for boundary layer control, 1998, ASME International Gas Turbine Congress, 98-GT-046.
10. JONES, K.D., CASTRO, B.M., MAHMOUD, O. and PLATZER, M.F. A numerical and experimental investigation of flapping-wing propulsion in ground effect, 2002, AIAA Paper No 2002-0866.
11. CARR, L.W. and CHANDRASEKHARA, M.S. Compressibility effects on dynamic stall, *Progress in Aerospace Sciences*,, 1996 **32**, pp 523-573.
12. MCCROSKEY, W.J. Unsteady airfoils, *Ann Rev Fluid Mech*, 1982, **14**, pp 285-311.
13. TUNCER, I.H., LAI, J.C.S. and PLATZER, M.F. A computational study of flow reattachment over a stationary/flapping airfoil combination in tandem, 1998, AIAA Paper No 98-0109.
14. CASTRO, B.M. Multi-block Parallel Navier-Stokes Simulations of Unsteady Wind Tunnel and Ground Interference Effects, 2001, PhD thesis, Department of Aeronautics & Astronautics, Naval Postgraduate School.
15. CYLINDER, D., SRULL, D. and KELLOGG, J. Biomorphic approaches to micro air vehicles, 2003, UAV Asia-Pacific 2003 Conference.
16. LAITONE, E.V. Wind tunnel tests of wings and rings at low Reynolds numbers, Chapter 5, *Fixed and Flapping Wing Aerodynamics for Micro Air Vehicle Applications*, AIAA Progress in Aerospace Sciences Series, MUELLER, T. (Ed), **195**, pp 83-90.
17. TORRES, G.E. and MUELLER, T.J. Aerodynamic characteristics of low aspect ratio wings at low Reynolds numbers, 2001, Chapter 7, *Fixed and Flapping Wing Aerodynamics for Micro Air Vehicle Applications*, AIAA Progress in Aerospace Sciences Series, MUELLER, T. (Ed), **195**, pp 115-142.
18. KORNBLUH, R. D., LOW, T. P., STANFORD, S. E., VINANDE, E., BONWIT, N., HOLEMAN, D., DELAURIER, J. D., LOEWEN, D., ZDUNICH, P., MACMASTER, M. and BILYK, D. Flapping-wing propulsion using electroactive polymer artificial muscle actuators, Phase 2: radio-controlled flapping-wing testbed, 2002, SRI International Report ITAD-3470-FR-03-009.
19. PAPADOPOULOS, J.P. An Experimental Investigation of the Geometric Characteristics of Flapping-wing Propulsion for a Micro Air Vehicle, 2003, Master's thesis, Department of Aeronautics & Astronautics, Naval Postgraduate School.
20. BRADSHAW, C.J. An Experimental Investigation of Flapping Wing Aerodynamics in Micro Air Vehicles, 2003, Master's thesis, Department of Aeronautics & Astronautics, Naval Postgraduate School.